



Phase formation during the decomposition of ammonium heptamolybdate — an in situ XAFS and XRD Investigation

J. Wienold, R.E. Jentoft, T. Ressler*

Department of Inorganic Chemistry, Fritz-Haber-Institute of the MPG, Faradayweg 4-6, 14195 Berlin, Germany

* Corresponding author: e-mail ressler@fhi-berlin.mpg.de, phone +49 30 8413 3192, fax +49 30 8413 4401

Accepted November 2002

Abstract

The decomposition of ammonium heptamolybdate was investigated by in situ XAFS and in situ XRD to elucidate the influence of different atmospheres on the products formed. The formation of different decomposition products and various intermediates is described in detail.

Keywords: in situ XAFS, molybdenum oxides, Ammonium Heptamolybdate

Introduction

Decomposition of ammonium heptamolybdate (AHM) can result in the formation of different molybdenum oxides, depending on the experimental conditions. These molybdenum oxides can serve as model systems for the much more complex mixed oxide systems $\text{Mo}_x(\text{V,W})_y\text{O}_{3-x}$, which are used extensively as partial oxidation catalysts for light alkenes. The structure of the catalytically active phase in these systems is still under debate (Gaigenaux *et al.*, 2000). Therefore, it is important to fully understand the different decomposition ranks of AHM to tailor the molybdenum oxide model systems formed in terms of, for instance, composition, crystallinity and particle size. However, the variety of products which can be obtained by the treatment of AHM under different atmospheres is not fully known yet. Although the decomposition of AHM has been studied to some extent in the past (Schwing-Weill, M.-J. (1967), Yong, W.J. (1990) (a selection)), no consistent mechanism exist. Hence, a detailed study on the influence of different parameters like reactant atmosphere or heating rate on the products and intermediates formed, is required. In this work, we investigated the decomposition of AHM in pure helium and in mixtures of helium with 20% oxygen and 5% hydrogen. In situ X-ray absorption spectroscopy (XAS) and in situ X-ray diffraction (XRD) are used to obtain structure information on the long range and short range order. Simultaneously, the composition of the gas phase is monitored by mass spectroscopy. In addition, the results obtained are compared to thermal gravimetry (TG) and differential thermal analysis (DTA) data.

Experimental

Starting material

Ammonium heptamolybdate tetrahydrate, AHM, $(\text{NH}_4)_4\text{Mo}_7\text{O}_{24} \cdot 4 \text{H}_2\text{O}$ (Aldrich, Analysis: total metallic impurities < 200 ppm) was used as purchased. Phase purity was verified by X-ray powder diffraction (ICSD, 27-472).

In situ X-ray Absorption spectroscopy

The in situ XAFS experiments were carried out at the Mo K edge (19.999 keV) at beamline X1.1 at the Hamburger Synchrotronstrahlungslabor, HASYLAB, using a Si(311) double crystal monochromator. A measuring time of 4.5 min / spectra resulted in a temperature range of ~ 22 K / spectra at a heating rate of 5 K/min. The AHM was mixed with Boron-Nitride (7 mg AHM / 30 mg BN, edge jump ~2 ?) and pressed into 5 mm in diameter self supporting pellets. A flow reactor of ~ 4 ml volume was used for the transmission XAFS measurements. Gas flow was controlled by Bronkhorst mass flow controller and the gas phase composition was monitored by mass spectroscopy (QMS 200, Pfeiffer). Temperature range was from 300 K to 770 K. Data reduction and analysis of the XAFS were carried out using the software WinXAS 2.0 (Ressler T., 1998). Spectra were energy calibrated to the spectrum of a molybdenum metal foil. Background subtraction and normalization were done using linear fits to the pre-edge and EXAFS region. The second inflection point in the edge was taken as the energy threshold, E_0 . The atomic absorption, μ_0 , was determined to minimize peaks with low (< 1 Å) R value in the Fourier transform while leaving the radial distribution function (RDF) unaffected. XAFS refinement was done in R space

using FEFF7 (Rehr et al., 1994) for calculating amplitudes and phases. Scattering paths were generated by FEFF7 using single crystal data.

In situ X-ray diffraction

In situ XRD studies were performed at a *Stoe STADI-P* diffractometer (Ge secondary monochromator, Cu K α radiation, Bragg-Brentano geometry), equipped with a *Bühler HDK S1* high temperature cell (400 ml). The system used for flow control and gas phase analysis was similar to that used for the XAFS experiments. In contrast to the XAFS measurements, during in situ XRD the temperature was kept constant every 25 K for the time of the measurement (1,5 h or 15 min).

TG/DTA study

Weight loss measurements (TG/DTA) were performed with a Seiko Instruments SSC/5200 (Pt-Rh 13% thermocouple), in pure nitrogen, 20 % Oxygen in helium and 5 % hydrogen in helium and a heating rate of 5 K/min. Total flow were 50 ml. Gas phase analysis was done with a *Pfeiffer QMS 200*, mass spectrometer.

Results and discussion

Decomposition in 20 % oxygen

Fig. 1 shows the evolution of the sample weight loss (TG/DTA) and the MS signals H $_2$ O and NH $_2$) during the decomposition in 20 % oxygen. The first decomposition step at 343 K results in a weight loss over a period of about 200 K. This step is accompanied by two DTA signals indicating endothermal processes. MS analysis shows loss of water for the first DTA signal and loss of water and ammonia for the second DTA signal. At 450.5 K an exothermic DTA signal is observed. The corresponding change in the slope of the TG curve is very small and observable only in the derivative. This signal is accompanied by an evolution of water and ammonia. At 525 K a distinct change in the slope of the TG-curve occurs accompanied by an endothermal DTA signal. Eventually, at 625 K the last step in the decomposition of AHM occur, which is accompanied by an exothermal DTA signal. At both steps loss of water and ammonia is visible.

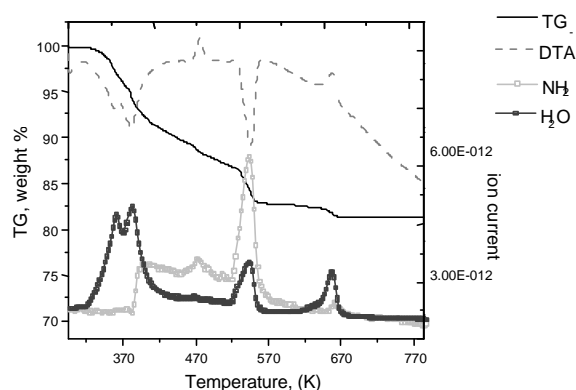


Figure 1

Evolution of weight loss during decomposition of AHM in 20 % oxygen together with MS signals for H $_2$ O and NH $_2$ (no axis inscription for the DTA signal).

Fig. 2 shows the evolution of XRD pattern during the decomposition of AHM in 20 % oxygen. Four distinct steps are visible. The first pattern at 320 K corresponds to

that of AHM. Between 370 and 420 K the patterns indicate a rapid decrease in crystallinity which results in an amorphous phase. This is referred to as the first step in the decomposition of AHM (TG/DTA, Fig. 1). At 510 K the formation of a new phase is observed which can be identified as a molybdenum oxide (NH $_3$ /H $_2$ O)(MoO $_3$) $_3$ with hexagonal structure. This correspond to the third step in the TG/DTA data. At 620 K a transition from the hexagonal phase to orthorhombic MoO $_3$ can be seen. The formation of orthorhombic MoO $_3$, can be assigned to the final decomposition step observed in the weight loss curve at 670 K. Interestingly the second step in the TG/DTA data has no corresponding step in the in situ diffraction data.

In fig. 3 the evolution of the EXAFS radial distribution function (RDF) during the decomposition of AHM in 20 % oxygen is shown. Between 373 and 473 K the RDF exhibits a pronounced decrease of amplitude of the shells higher than 2 Å. This decrease indicates a loss of structural order in agreement with the amorphous phase observed in the XRD data. At 496 K the formation of a new phase is observed. In contrast to the XRD data no change is visible at 620 K which may indicate the formation of a new phase. This is surprising, taking into account the distinct structural long range differences between the hexagonal phase and the orthorhombic MoO $_3$. However, a detailed look into the pair distribution functions of the two phases

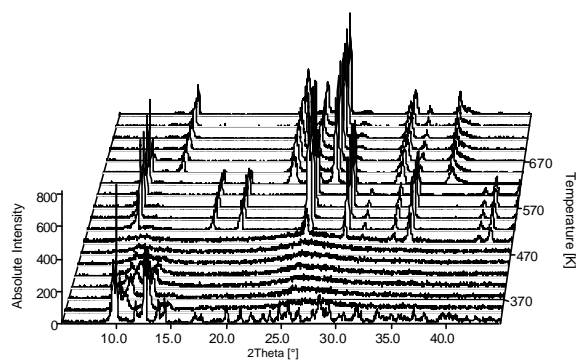
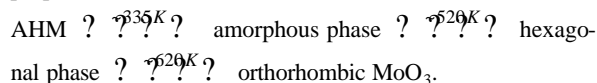


Figure 2

Evolution of X-ray diffraction pattern during decomposition of AHM in 20 % oxygen.

reveals a very similar short range order and explain the apparent absence of a distinct phase transformation in the XAFS data. This is corroborated by XAFS refinements of the two model systems to the experimental spectra which afford similar distances and fit residuals. In the temperature range from 496 K to 771 K no significant change in bond length or Debye temperatures is visible which indicates a phase transformation. Hence for the decomposition of AHM in 20 % Oxygen the following scheme, labeled scheme 1, is proposed:



Decomposition in helium

The decomposition of AHM in helium follows decomposition scheme 1 with only one difference. Instead of MoO $_3$ the formation of a mixture of Mo $_4$ O $_{11}$ and MoO $_3$ is observed. Apparently, an amorphous Mo $_4$ O $_{11}$ form occur at 620 K, which seem to crystallize with increasing temperature. In fig. 4 in situ XRD data and RDF of the decomposition of AHM in helium, with range from 620 K to 820 K is shown. From the XRD data it can be seen that the increase in the amount of Mo $_4$ O $_{11}$ is not accompanied by a decrease in the peak intensity of MoO $_3$. The EXAFS RDF exhibits no distinct changes within the corresponding temperature range.

This indicates a constant ratio of the two phases MoO_3 and Mo_4O_{11} , whereas the Mo_4O_{11} occurs in an amorphous form at 620 K and there is only a long-range ordering proceeding in the temperature range from 620 K to 820 K.

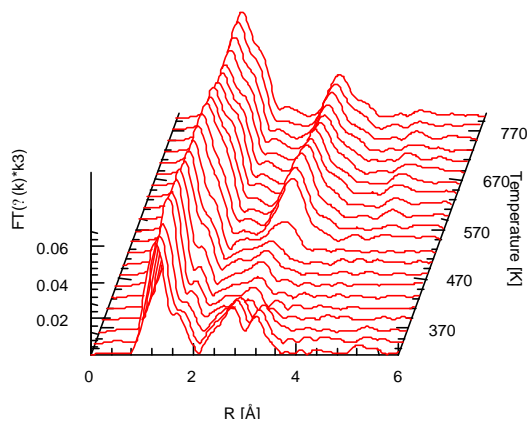


Figure 3

Evolution of radial distribution function during decomposition of AHM in 20 % oxygen.

Decomposition in 5 % hydrogen

The decomposition of AHM in 5% hydrogen proceeds not via scheme one but a very similar scheme. Instead of the formation of the hexagonal phase at 520 K, directly orthorhombic MoO_3 is observed, which is reduced at 650 K into MoO_2 . The diffraction data of the MoO_3 formed shows a strong preferred orientation, probably because of the formation of platelets with the (110) face as the main face.

Formation of Ammonium Tetramolybdate

In the in situ XRD and XAFS data no phase formation or structural change was observed which may correspond to the second decomposition step in the TG/DTA at about 460 K.

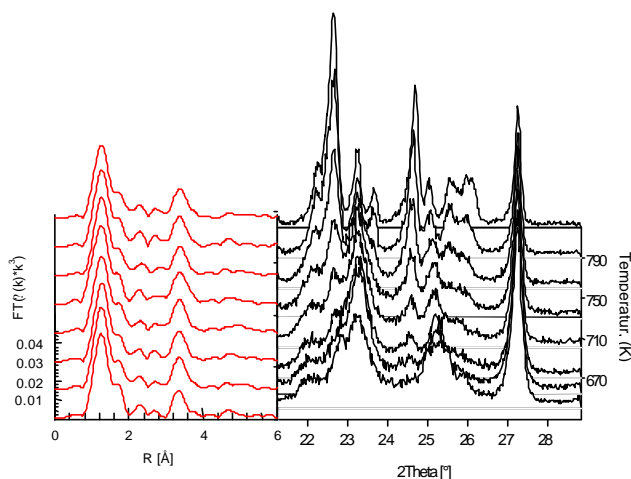


Figure 4

Assembling of X-ray-diffraction pattern and radial distribution function from 620 K to 820 K during decomposition of AHM in helium (no axis inscription for absolute intensities of the XRD data)

By isothermal treatment of AHM at 460 K for more than 24 h it was possible to produce a well crystallized phase which could be identified as $(\text{NH}_3)_2\text{Mo}_4\text{O}_{13}$, ammonium tetramolybdate (ATM), by XRD analysis (ICSD 68-562). However, the decomposition of this compound is different from that of

AHM. During the decomposition of ATM, at 570 K a phase mixture of the hexagonal phase and MoO_3 is formed. At 620 K the hexagonal phase decompose into MoO_3 and amorphous Mo_4O_{11} . In Fig. 5 the RDF of ATM and the amorphous phase formed during the decomposition of AHM at 500 K is shown. The very good agreement between the two RDF indicate that the amorphous phase in Fig. 2+3 is indeed closely related to ATM. Apparently disordered ATM is formed during the decomposition of AHM, but its crystallization is inhibited.

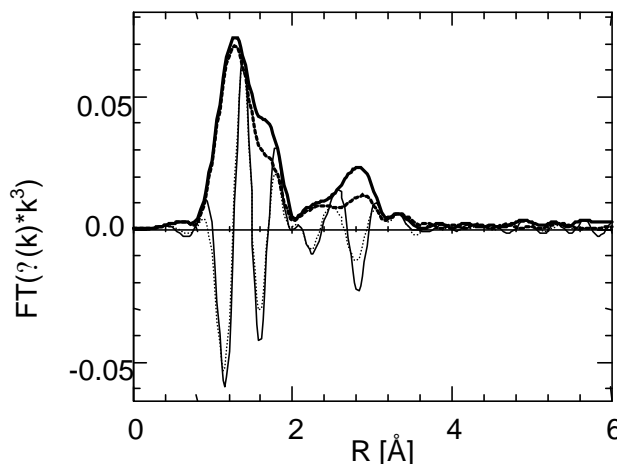


Figure 5

Radial distribution function of the amorphous phase at 500 K (Fig. 2+3) during the decomposition of AHM in helium (···) and RDF of ammonium tetramolybdate (—) together with the imaginary parts of the Fourier transform.

Conclusion

The combination of the two complementary methods X-ray diffraction and in situ XAFS permits a detailed study of the various phases formed during the decomposition of AHM.

From the results presented for the decomposition in three different atmospheres it can be seen that the reactant atmosphere and the heating rate have a distinct influence on the products and on the decomposition mechanism.

We acknowledge the *Hamburger Synchrotronstrahlungslabor* HASYLAB for providing beamtime for this work. The authors are grateful to Professor R. Schlögl for valuable discussions and continuous support. T. Ressler thanks the Deutsche Forschungsgemeinschaft “DFG” for financial support (Habilitationstipendium).

References

- Gaigneaux E. M.; Genet M. J.; Ruiz P.; Delmon B. (2000). *J. Phys. Chem. B* **104**, 5724-5737
- Rehr, J.J.; Booth, C.H.; Bridges, F.; Zabinsky, S.I. (1994). *Phys. Rev. B* **49**, 12347-12352
- Ressler T. (1998). *Synch. Rad.* **5**, 118-?
- Schwing-Weill, M.-J. (1967). *Bull. Soc. chim.* **10**, 3795-3798
- Yong, W.J. (1990). *Thermochimica Acta* **158**, 183-186